

Weaker Ligands Can Dominate an Odor Blend due to Syntopic Interactions

Daniel Münch¹, Benjamin Schmeichel¹, Ana F. Silbering² and C. Giovanni Galizia¹

¹Neurobiology, University of Konstanz, D-78457 Konstanz, Germany and ²Center for Integrative Genomics, University of Lausanne, CH-1015 Lausanne, Switzerland

Correspondence to be sent to: Daniel Münch, Neurobiology, University of Konstanz, D-78457 Konstanz, Germany. e-mail: daniel.muench@uni-konstanz.de

Accepted December 3, 2012

Abstract

Most odors in natural environments are mixtures of several compounds. Perceptually, these can blend into a new “perfume,” or some components may dominate as elements of the mixture. In order to understand such mixture interactions, it is necessary to study the events at the olfactory periphery, down to the level of single-odorant receptor cells. Does a strong ligand present at a low concentration outweigh the effect of weak ligands present at high concentrations? We used the fruit fly receptor dOr22a and a banana-like odor mixture as a model system. We show that an intermediate ligand at an intermediate concentration alone elicits the neuron’s blend response, despite the presence of both weaker ligands at higher concentration, and of better ligands at lower concentration in the mixture. Because all of these components, when given alone, elicited significant responses, this reveals specific mixture processing already at the periphery. By measuring complete dose–response curves we show that these mixture effects can be fully explained by a model of syntopic interaction at a single-receptor binding site. Our data have important implications for how odor mixtures are processed in general, and what preprocessing occurs before the information reaches the brain.

Key words: *Drosophila melanogaster*, mixture interaction, mixture processing, olfaction, olfactory receptor neuron, Or22a

Introduction

Naturally occurring odors usually consist of tens or even hundreds of different components at varying concentrations (Knudsen et al. 1993). Depending on the olfactory receptor (OR) it expresses, an olfactory receptor neuron (ORN) is able to respond to a large set of odorants (Hallem et al. 2004). Odor response profiles overlap, thereby leading to an ensemble of activated ORNs upon odorant presentation (de Bruyne et al. 2001; Hallem and Carlson 2006; Galizia et al. 2010). Because even a single ligand is able to elicit an ensemble response across ORNs, in a mixture, the ensemble responses of the different components overlap and generate a novel mixture activation pattern (Johnson et al. 2010). On a perceptual level, humans have difficulties to recognize individual components with increasing mixture complexity and instead perceive the stimulus as a new odor quality (Jinks and Laing 2001). In other cases, honeybees have been shown to learn odor mixtures *via* selection of only a few key components (Reinhard et al. 2010). These, and similar, mixture effects are thought to derive from mixture interactions in odor coding. In the brain network, the overlapping input channels influence each other laterally *via* neural circuits,

resulting in mixture interactions (Silbering and Galizia 2007; Lei and Vickers 2008; Olsen and Wilson 2008; Root et al. 2008; Ignell et al. 2009). The presence of one component might for example suppress the response to the other (suppression or hypoaddivity) or enhance it (synergism; Duchamp-Viret et al. 2003; Silbering and Galizia 2007; Kuebler et al. 2011).

However, mixture interactions can also be found prior to any brain network at a single ORN level in the olfactory periphery (Cromarty and Derby 1998; Duchamp-Viret et al. 2003; Rospars et al. 2008; Hillier and Vickers 2011). Thus, these effects directly shape the sensory input the brain receives. Studying the mechanisms underlying mixture interactions in the periphery is therefore important to understand how natural odors are perceived.

Here, we measured odor-evoked calcium responses in the dendrites and somata of *Drosophila* ORNs. We used the well-characterized receptor dOR22a (Pelz et al. 2006; Galizia et al. 2010), which responds strongly to banana extract (Hallem and Carlson 2006), and an artificial banana-like odor blend (Jordán et al. 2001), which allowed us to

dissect the contribution to the odor response of different components. As not only the quality of components but also their relative concentration is an important feature of a mixture, we used different concentrations and recorded full dose–response curves. We found that mixture responses are hypoadditive in dOR22a. Responses to odor-concentration series demonstrate that the observed hypoadditivity is likely due to syntopic interactions at a single-odorant receptor-binding site (Rospars et al. 2008). Thus, a relatively simple peripheral mechanism already explains a large part of mixture interactions that render odor mixtures unique and identifiable “perfumes.”

Materials and methods

We recorded odor-evoked responses in dOr22a ORNs using Ca^{2+} imaging. In each animal, up to 31 stimulus responses were recorded aiming at 1) screening for responses toward 15 selected banana-scent components, 2) measuring mixture interactions, or 3) characterizing full dose–response curves. All measurements were performed at the same experimental setup using the same strain of flies. A total of 40 animals were used for this study.

Animals

Flies were kept at 25 °C in a 12/12 light/dark cycle. Animals were reared on standard medium (100 mL contain 2.2 g yeast, 11.8 g of sugar beet syrup, 0.9 g of agar, 5.5 g of cornmeal, 1 g of coarse cornmeal, and 0.5 mL of propionic acid). Female *Drosophila melanogaster* were used for experiments 1–3 weeks after eclosion. Flies were of genotype P[UAS:GCaMP];P[Gal4:dOr22a]/CyO, expressing the Ca^{2+} reporter G-CaMP 1.3 in dOr22a-bearing cells (crossed from wP[UAS:G-CaMP];CyO/Sp;+ flies provided by Jing Wang, University of California, San Diego, La Jolla, CA; Nakai et al. 2001; Wang et al. 2003).

Flies were mounted in custom-made holders, placed with their neck into a slit; the head was fixed to the holder with a drop of dental glue (Tetric EvoFlow, Ivoclar Vivadent, Ellwangen, Germany). A half electron microscopy grid was placed on top of the head, stabilizing the antenna by touching the second but not the third antennal segment.

Odorant preparation

Odorants were purchased from Sigma–Aldrich in the highest purity available (Table 1). Pure substances were diluted in 5 mL mineral oil (Sigma–Aldrich, Steinheim, Germany), dilutions ranged from 10^{-2} to 10^{-8} . Odors were prepared in 20–mL headspace vials sealed with a Teflon septum (Axel Semrau, Germany).

Information and abbreviations for all odorants used are given in Table 1, the tested mixtures were MIX15 (all 15 components: 1-butanol [BO], 1-hexanol [HO], 2-pentanol [PO],

Table 1 Table of odorants and concentrations used in the experiments together with their Chemical Abstracts Service (CAS) number and the abbreviated code used in the text

CODE	Name	CAS	ppm	Dilution	Class
HE	E-2-hexenal	6728-26-3	32.2	$10^{-3.9}$	Aldehyde
HL	Hexanal	66-25-1	21.47	10^{-4}	Aldehyde
BN	3-hydroxy-2-butanon	513-86-0	20.33	$10^{-3.5}$	Ketone
PO	2-pentanol	6032-29-7	14.26	$10^{-3.8}$	Alcohol
MO	3-methyl-1-butanol	123-51-3	7.9	$10^{-3.6}$	Alcohol
IAB	Isoamyl butyrate	106-27-4	7.13	$10^{-3.1}$	Ester
IA	Isopentyl acetate	123-92-2	4.85	$10^{-4.3}$	Ester
PN	2-pentanone	107-87-9	2.71	$10^{-5.6}$	Ketone
IBA	Isobutyl acetate	110-19-0	2.45	$10^{-5.2}$	Ester
BA	Butyl acetate	123-86-4	1.32	$10^{-5.3}$	Ester
HO	1-hexanol	111-27-3	1.17	$10^{-3.8}$	Alcohol
BO	1-butanol	71-36-3	1.06	10^{-5}	Alcohol
BB	Butyl butyrate	109-21-7	0.83	$10^{-4.8}$	Ester
HA	Hexyl acetate	142-92-7	0.57	$10^{-4.9}$	Ester
EB	Ethyl butyrate	105-54-4	0.15	$10^{-6.4}$	Ester

2-pentanone [PN], 3-hydroxy-2-butanon [BN], 3-methyl-1-butanol [MO], butyl acetate [BA], butyl butyrate [BB], E-2-hexenal [HE], ethyl butyrate [EB], hexanal [HL], hexyl acetate [HA], isoamyl butyrate [IAB], isobutyl acetate [IBA], and isopentyl acetate [IA]); MIX4 (IA, BA, EB, and PO); MIX3 (BA, EB, and PO); IA.BA (IA and BA); IA.EB (IA and EB); and IA.PO (IA and PO).

Odorant dilutions for the artificial banana blend and its components were prepared in order to match the concentrations appearing in natural banana fruit reported by Jordán et al. (2001). For producing the desired headspace concentrations in ppm, the corresponding vol/vol dilutions in mineral oil were estimated using the published information about the relation of liquid- and vapor-phase concentrations of volatile compounds in mineral oil (Cometto-Muñiz et al. 2003) and interpolating based on available vapor-pressure information (Pelz 2005; Pelz et al. 2006).

For dose–response curves pure odorants were diluted in mineral oil in decadic steps from 10^{-2} to 10^{-8} , headspace concentrations in ppm were calculated as explained above. The ratios of the single components within the binary mixtures were 1:1 (vol/vol), which corresponds to the following ppm ratios in the headspace: $ratio_{PO/IA} = 0.78$ and $ratio_{EB/IA} = 3.34$.

Compound concentrations in all mixtures are the same as in single odors, for example, mixture AB contains A + B and not 0.5 A + 0.5 B.

Stimulus application

A computer-controlled autosampler (PAL, CTC Switzerland) was used for automatic odor application. A headspace of 2 mL was injected in two 1 mL portions at time points 6 s and 9 s with an injection speed of 1 mL/s into a continuous flow of purified air flowing at 60 mL/min. The stimulus was directed to the antenna of the animal *via* a Teflon tube (inner diameter 2 mm, and length 39.5 cm).

The interstimulus interval was approximately 2 min. Solvent control, room air control, and reference odorant were measured after every 7 or 8 stimuli (1 block). The autosampler syringe was flushed with purified air for 30 s after each injection. After each block of stimuli, the syringe was washed with hexane (Merck, Darmstadt, Germany), heated up to 48 °C, and rinsed with continuous clean air for 6 min.

Gas chromatography

A gas chromatography–mass spectrometry system (GC–MS, Trace GC Ultra & DSQ II, Thermo Fisher Scientific, equipped with a 60 m × 0.25 mm forte bpx5 nonpolar capillary column, SGE International, Australia) was used to measure headspace concentrations of compounds in mixtures and single compounds. Headspace of 1 mL was injected with an autosampler (PAL, CTC, Switzerland), the GC run started at 40 °C and increased 10 °C/min up to 250 °C. MS profile identification and GC peak measurement was performed in Xcalibur (Thermo Fisher Scientific).

Ca²⁺ imaging

Ca²⁺ imaging was performed with a fluorescence microscope (BX51WI, Olympus, Tokyo, Japan) equipped with a ×50 air lens (Olympus LM Plan FI 50×/0.5). A CCD camera (TILL Imago, TILL Photonics, Gräfelfing, Germany) was mounted on the microscope recording with 8 × 8 pixel on-chip binning resulting in 80 × 60 pixel sized images. For each stimulus recordings of 20 s at a rate of 4 Hz were performed using TILLvisION (TILL Photonics, Gräfelfing, Germany).

A monochromator (Polychrome II, TILL Photonics, Gräfelfing, Germany) produced excitation light of 470 nm wavelength that was directed onto the antenna *via* a 500 nm low-pass filter and a 495 nm dichroic mirror, emission light was filtered through a 505 nm high-pass emission filter.

Data analysis

Data were analyzed in custom written routines using IDL (ITT VIS), R (<http://www.r-project.org>), and LibreOffice (<http://www.libreoffice.org>). Statistics were done in SigmaStat (Systad Software).

Animals that showed stable responses to the reference odor (ethyl propionate) throughout the experiment were included into the analysis. Recorded movies were manually

corrected for movement artifacts, and an area of interest was defined for the parts of the antenna that showed fluorescence increase upon stimulation. All calculations were done within that area.

Relative fluorescence change was calculated as $\Delta F/F = ((F_i - F_0)/F_0) \times 100$ with F_i being the fluorescence at *frame*_{*i*} and F_0 being the mean fluorescence of 19 frames before stimulus onset.

We corrected for bleaching artifacts by fitting a logarithmic function for frames 4–22 and 70–80 to the ΔF trace leaving out 12 s after stimulus onset and weighting frames 4–22, 3-fold compared with after-response end (see [Silbering and Galizia 2007](#) for details).

The response amplitude was calculated as the average of 3 frames around the response maximum within 2 s after stimulus onset.

To compare across animals, responses were normalized as follows: within each animal response to solvent control was set to 0 and response to reference odor ethyl propionate was set to 1. Because responses decrease over time, all other responses were calculated by linear interpolation.

A Hill function as shown in Formula 1 was fitted to the concentration series of odors using the CURVEFIT function in IDL ([Sachse and Galizia 2003](#); [Pelz et al. 2006](#)). The obtained parameters of the single odor-concentration series (*hill* [slope], *Rmax* [maximum response], and *EC50* [concentration eliciting the half maximal response]) were used to predict the mixture parameters according to [Rosparis et al. \(2008\)](#). The Hill parameter (slope) was estimated from the best 2 fits within an animal.

$$R(x) = \frac{x^{\text{hill}}}{x^{\text{hill}} + EC50^{\text{hill}}} \times Rmax. \quad (1)$$

Response estimation

Two models for binary mixture response prediction were compared with our data. [Tabor et al. \(2004\)](#) used the measured responses to the single and double concentration of the individual compounds to gather local information on their dose–response curves. The logic is that if a stimulus A elicits a response, adding molecules of B to it that are also excitatory should increase the response, if we assume that no interaction happens between the odorants. Mathematically, a mixture response can be estimated using a “linear interpolation” of this local dose–response data.

$$R_{pred} = \max_{1x}(R_A, R_B) + \sqrt{\Delta_{2x-1x} R_A \times \Delta_{2x-1x} R_B}. \quad (2)$$

With R_{pred} , R_A , and R_B being the predicted response and the responses toward odorant A and B, respectively. For the purpose of this study, we define a measured response that differs from this prediction as a mixture interaction.

[Rosparis et al. \(2008\)](#) argue that if the 2 substances A and B interact with the same binding pocket of interaction site,

then the presence of molecules B in addition to A will interfere with the response. In order to predict this syntopic interaction mathematically, it is necessary to know the complete dose–response curve for both mixture components. The model then predicts the parameters $EC50$ and $Rmax$ of the dose–response curves for the mixtures as:

$$EC50_{pred} = (1+r)EC50_A EC50_B \sqrt[n]{\frac{1}{r^n EC50_B^n + EC50_A^n}}. \quad (3)$$

$$Rmax_{pred} = \frac{Rmax_A r^n EC50_B^n + Rmax_B EC50_A^n}{EC50_A^n + r^n EC50_B^n}. \quad (4)$$

With r being the ratio of the 2 components, n being the Hill value, $EC50$ the dose that elicits the half maximal response, and $Rmax$ the maximum response a ligand elicits. It is important to note that this model only works with concentrations measured as molecular concentrations in ppm and not for dilution units.

Results

Which odor component does dOr22a respond to when a banana-like mixture is presented?

The *D. melanogaster* olfactory receptor dOr22a is an especially well-described receptor that is tuned to fruity odors and strongly activated by banana (de Bruyne et al. 2001; Dobritsa et al. 2003; Stensmyr et al. 2003; Hallem and Carlson 2006; Pelz et al. 2006). Interestingly, when comparing the dOr22a response profile to the aromatic profile of banana fruit (Jordán et al. 2001), we recognized that the most abundant banana component HE is only a weak ligand, whereas the low concentrated EB strongly activates dOr22a (Figure 1A).

In order to analyze the role of single components in the banana blend response, we created an artificial banana mixture containing 15 prominent components from banana scent (MIX15). We used published data about the relationship between liquid- and vapor-phase concentrations (Cometto-Muñiz et al. 2003) to prepare the single banana components and their mixture by diluting odorants in mineral oil in a way that vapor-phase concentrations matched those of the aromatic banana profile reported by Jordán et al. (2001; Table 1).

We performed GC–MS analyses of MIX15 and the single components alone to exclude possible interactions at a chemical level that could prevent compounds from evaporation. For those peaks that were detectable, we could show that the GC–MS peak areas were the same whether diluted individually or in the mixture. Figure 1C shows the GC–MS measurement for the mixture overlaid with those of IA and PO alone (see online supplementary Figure S1 for comparison of all detected peaks).

dOr22a responds to many components in the mixture

We performed Ca^{2+} imaging of sensory neuron dendrites using the Ca^{2+} indicator G-CaMP (Nakai et al. 2001) in dOr22a neurons. The mixture MIX15 and 5 of the 15 components elicited responses that were significantly different from the solvent control (mineral oil (MOL); Figure 1B). The artificial banana blend lead to the strongest activation followed by IA, EB, IBA, BA, and PO (Kruskal–Wallis, $P < 0.001$; multiple comparisons vs. control group, Dunn's method, $P < 0.05$).

Mixture responses are hypoaddivitive

We compared the responses elicited by the 5 active components from above to those elicited by the complete 15-component mixture. The response of dOr22a toward IA alone was not different from the response elicited by the complete mixture that was very surprising as there were at least 4 other active compounds in the mixture (Kruskal–Wallis, $P < 0.001$; multiple comparisons vs. control group, Dunn's method, $P < 0.05$). We therefore asked whether IA somehow suppresses the activity of the other mixture components.

Out of the effective banana components, we selected the 2 at lowest concentration (EB and BA) and the most abundant (PO) for the creation of binary mixtures with IA. We also composed 1 mixture containing all 3 components (MIX3) and 1 mixture containing the 3 components and IA (MIX4). Again we performed Ca^{2+} imaging of dOr22a ORNs on the antenna of *D. melanogaster* with the odors at their natural banana blend concentration (Figure 2A). IA and MIX15 gave the same responses, and all the other responses of mixtures containing IA as a component did not differ from IA alone. Interestingly the response elicited by MIX3 was almost as high as the response of the IA containing mixtures, producing a higher dOr22a response than its components alone.

Responses to binary mixtures A.B can be grouped in 3 types: suppressive, when the mixture response is lower than the response toward the stronger component A; hypoaddivitive, when the mixture response is equal to the stronger component A; synergistic, when the mixture response is higher than the response to substance A at the mixture concentration [A+B] (Duchamp-Viret et al. 2003; Silbering and Galizia 2007; Figure 3).

Assuming no interaction, responses to binary mixtures can be interpolated along the dose–response curves of the single components, sometimes misleadingly referred to as “linear summation”. This has been elaborated by Tabor et al. (2004) who derived Formula 2 for an expected mixture response (see Materials and Methods).

We predicted mixture responses for the 3 binary mixtures from measurements of the single and double concentrations of their components using Formula 2. We found the measured responses to be significantly lower than the predictions in all cases (Figure 2B; Wilcoxon signed rank test,

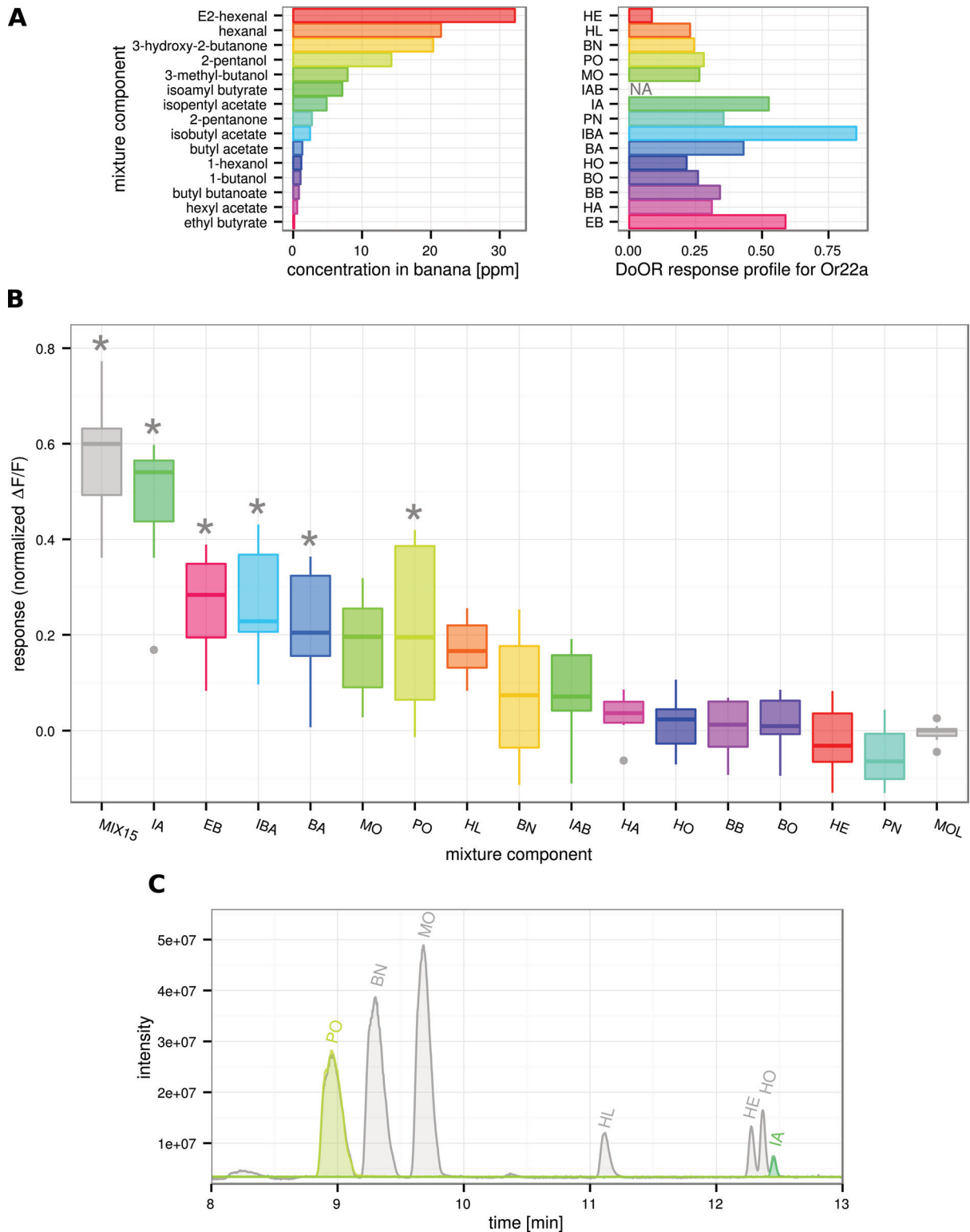


Figure 1 Selected banana compounds tested on dOr22a. **A** Barplot on the left is showing the concentration in ppm of 15 compounds as they appear in the aromatic profile of banana fruit (Jordán et al. 2001), barplot on the right is giving the corresponding response profile of dOr22a as in the DoOR database (Galizia et al. 2010). **B** Boxplot showing Ca^{2+} imaging data recorded on the antenna of *Drosophila melanogaster*, responses are normalized to ethyl propionate and shifted by mineral oil solvent (MOL) within each animal. Asterisks indicate significant responses compared with solvent MOL (Kruskal–Wallis/Dunn’s multiple comparisons vs. solvent group, $P < 0.05$, $n = 8-9$). Five of the components elicited a significant response when given alone. **C** Sample GC traces for MIX15 (gray), PO and IA. Traces of mixture and single component overlap their respective peaks. For abbreviations and odor concentrations/dilutions see Table 1. Boxplot shows median, lower, and upper quartile, whiskers extend to lowest and highest value that lies within 1.5 times the interquartile range from the box.

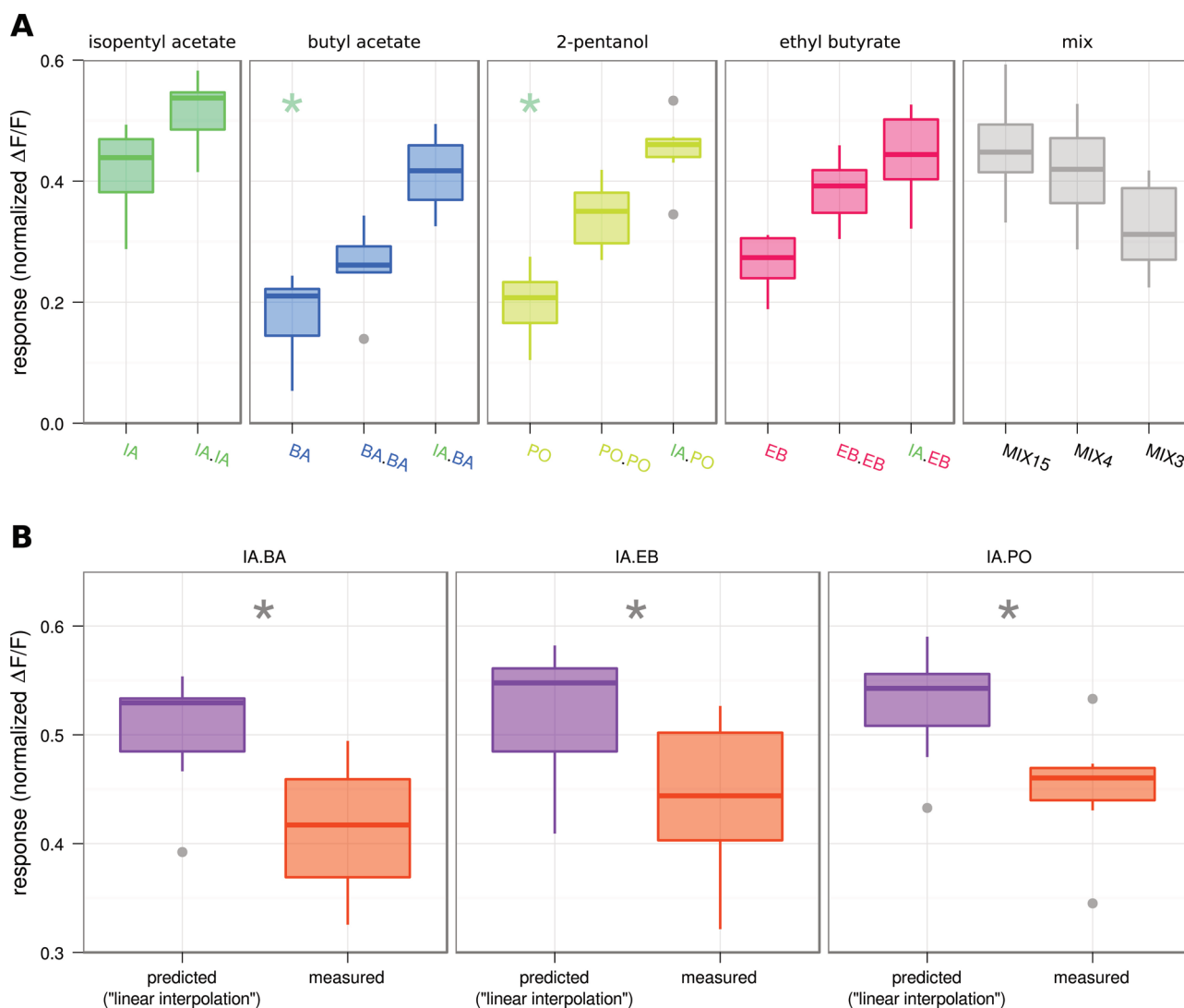


Figure 2 Binary mixtures with IA. **A** Boxplot comparing mixture components in single concentration (concentration as from banana profile, left in each panel), double concentration (second plot in each panel), the binary mixtures with IA (third plot in panels 2–4), and responses to different submixtures containing 15, 4, or 3 components (panel 5). No difference could be found between IA and the IA containing binary mixtures or between IA and the different multi component mixtures (MIX15: all 15 tested compounds; MIX4: IA, BA, EB and PO; MIX3: MIX4 without IA) (Kruskal–Wallis/Dunn’s multiple comparisons vs. control group, $P < 0.001$, $n = 7$). **B** Boxplot of responses to binary mixtures as predicted assuming no interactions (“linear interpolation”, purple) and as measured (orange). Prediction and measurement was significantly different in all cases (Wilcoxon Signed Rank Test, $P < 0.05$, $n = 7$). Boxplots show median, lower and upper quartile, whiskers extend to lowest and highest values that lie within 1.5 times the interquartile range from the box. This figure appears in color on the online version of this issue.

$P < 0.05$). Thus, all responses to mixtures were hypoadditive. Specifically, adding a component to IA as stimulus—even if a good ligand—did not contribute to the response.

Mixture components compete at receptor level

Given that the observed mixture interactions already occurred at receptor cell level, we further tested for syntopic interaction at the receptor-binding site. Syntopic interaction describes the competition of 2 ligands for binding to the same or at 2 overlapping binding sites on the same receptor (Neubig et al. 2003). The model from Rospars et al. (2008) assumes

a two-step mechanism of ligand binding and receptor activation and predicts a mixture dose–response curve from the dose–response curves of its components (Formulas 3 and 4).

We measured dose–response curves for PO and EB (the highest and the lowest concentrated component of our artificial banana blend), for IA and for their binary mixtures IA.PO and IA.EB. Pure odorants were diluted in mineral oil in decadic steps from 10^{-2} to 10^{-8} , and a Hill function was fitted to the data.

PO was a weaker ligand for dOr22a than IA, showing a lower efficiency (eliciting a lower maximum response, R_{max} , 0.67 compared with 0.94) and a lower affinity (a higher EC_{50}

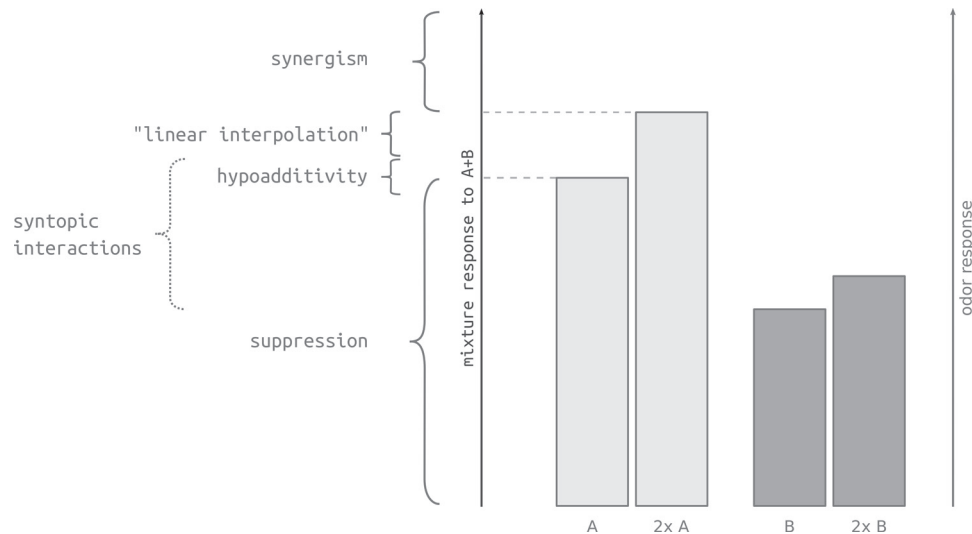


Figure 3 Scheme of mixture interaction types. Note that different authors use different wording and ranges according to different interaction mechanisms. A mixture response is termed suppressive when it is lower than the response toward the stronger component (A); hypoaddivity, when the mixture response is equal to the stronger component (A); synergistic, when the mixture response is higher than the response to the stronger component A at the mixture concentration [A+B] (“2x A” in the figure because in this figure we consider the case of [A] = [B] for simplicity). “Linear interpolation” refers to the case where no interactions happen and the response can be calculated according to Formula 2. Syntopic interaction at the receptor level generally results in responses within the upper suppression range but cannot be calculated precisely without knowledge of the full dose–response curves (Formulas 3 and 4).

value, 32.73 ppm compared with 7.26 ppm; **Figure 4A**). The mixture of both in the ppm ratio measured here ($\text{ratio}_{\text{PO/IA}} = 0.78$) followed the stronger component IA. EB on the other hand was a much stronger ligand for dOr22a than IA, showing a higher affinity (EC_{50} of 36.47 ppm compared with 67.92 ppm) and higher efficiency (R_{max} of 1.63 compared with 0.95; **Figure 4B**). Their mixture IA.EB also followed the stronger ligand, EB in this case ($\text{ratio}_{\text{EB/IA}} = 3.34$). Note that IA EC_{50} and R_{max} values differed slightly as the data were obtained in 2 different data sets in different seasons. We could not investigate this seasonal effect in this study.

The mixture dose–response curves in **Figure 4A** and **B** are located between their component curves, indicating the presence of syntopic interaction. Using the model of syntopic interaction to derive a mixture dose–response curve from the component curves leads to a very accurate prediction of the actually measured mixture dose–response curves (IA.PO: predicted EC_{50} : 8.59 ppm, measured EC_{50} : 8.55 ppm, predicted R_{max} : 0.88, measured R_{max} : 0.87; IA.EB: predicted EC_{50} : 25.28 ppm, measured EC_{50} : 38.9 ppm, predicted R_{max} : 1.44, measured R_{max} : 1.6; **Figures 4C** and **D**). Thus mixture interactions in IA.PO and IA.EB are fully accounted for by the ligands competing for the same dOr22a receptor-binding site.

Syntopic interaction applies for natural concentration ratios

The prediction of the mixture dose–response curves in **Figure 4** is based on diluting the pure odorants in decadic

steps and mixing them 1:1 (vol/vol), which translates to ratios of $\text{ratio}_{\text{PO/IA}} = 0.78$ and $\text{ratio}_{\text{EB/IA}} = 3.34$, respectively, when transformed to ppm in headspace after **Cometto-Muñiz et al. (2003)**. As we could show that our data can be described by the model of syntopic interaction, we calculated the mixture dose–response curves for the ratios in which the components occur in banana fruit ($\text{ratio}_{\text{PO/IA}} = 2.94$; $\text{ratio}_{\text{EB/IA}} = 0.031$, **Figure 5**). With the component dose–response curves we were also able to calculate a dose–response curve according to the “linear interpolation” model (**Figure 5**).

When calculating the syntopic interaction model using the natural banana fruit ratio of IA and PO, the mixture dose–response curve moved toward PO (its concentration in the mixture was much higher); however, it still remained closer to IA (dashed purple line in **Figure 5A**). The “linear interpolation” model (dotted purple line in **Figure 5A**) and the syntopic interaction model gave the same curves at lower concentrations; for higher concentrations, the interpolation model started deviating till it reached the same R_{max} level as the stronger component, whereas syntopic interaction followed the measured curve.

Using EB at the low concentration present in banana, the mixture curve for the syntopic model followed the IA curve closely. Like the models for IA.PO, the 2 models for IA.EB looked the same at the lower concentrations, but in the higher concentrations, the “linear interpolation” model deviated toward the stronger component, leading to a kink in the IA.EB curve (**Figure 5B**), whereas syntopic interaction created a smooth sigmoidal curve.

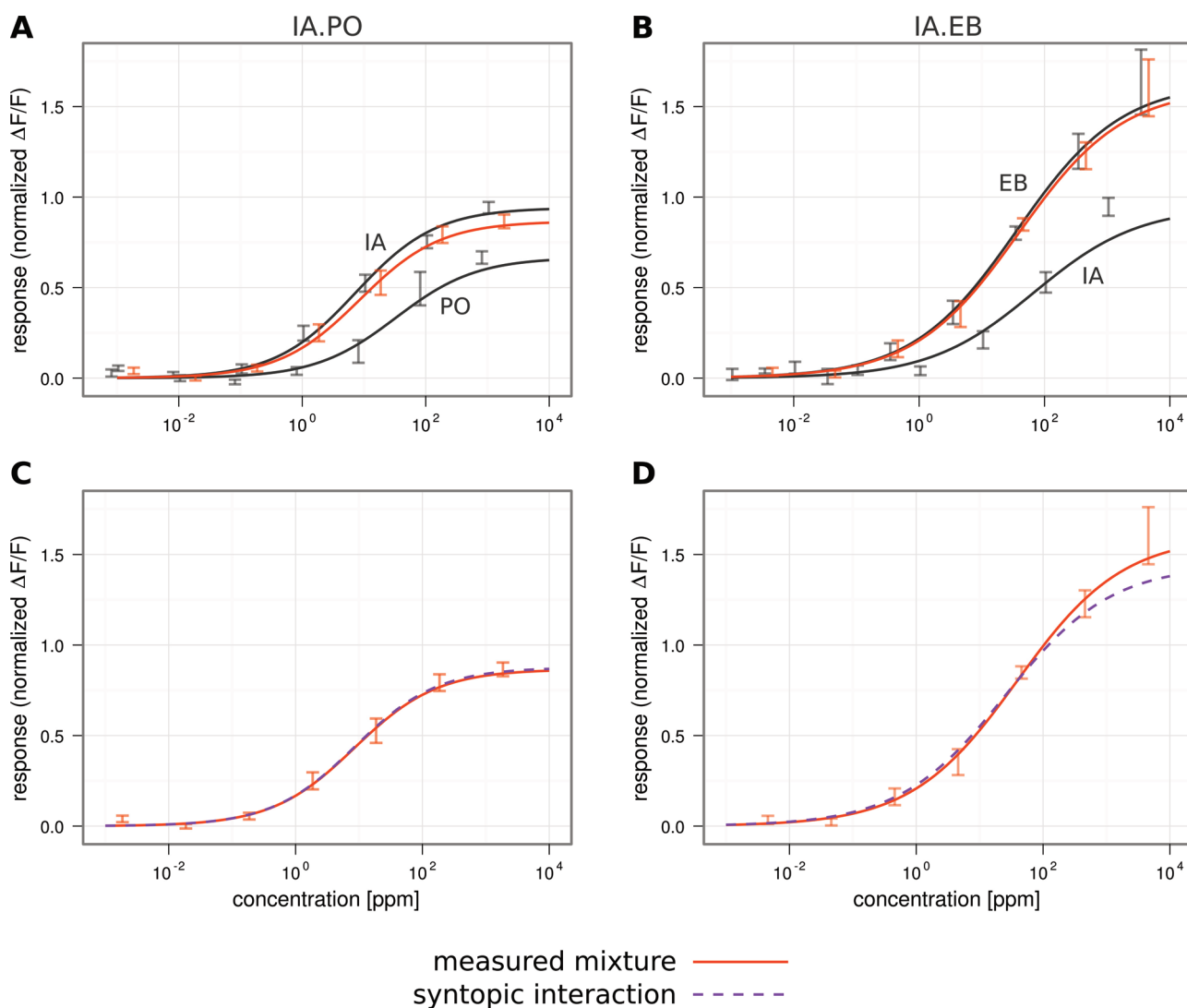


Figure 4 Dose–response curves for the single odorants IA and PO or EB (dark gray), and the binary mixtures IA.PO (orange) and IA.EB (orange). **A** and **B** All dose–response curves can be fitted by the Hill equation. **C** and **D** Overlay of the measured mixture responses (orange) and the modeled mixture following syntenic interaction (dashed purple; Rospars et al., 2008). The model is a good estimate of the data. Error bars indicate standard error mean; $n = 7$. This figure appears in color on the online version of this issue.

IA is the dominant banana-odor component for 22a

For IA and PO at the banana ratio, IA presented alone elicited the stronger responses from dOr22a across the whole concentration range (dashed gray lines in Figure 5A and B). For a better visualization we shifted the x axis in Figure 5C and D in a way that corresponding component and mixture concentrations are aligned horizontally. When comparing IA with EB, IA would elicit the stronger responses only at lower concentrations but EB would overtake at some point, leading to a kink in the “linear interpolation” model (Figures 5B and D).

However, in the syntenic interaction model the mixture follows IA closely, preserving a stable dose–response curve across concentrations and accounting for IA as the dominant mixture component for both binary mixtures.

Discussion

Mixture interactions at the periphery of olfactory systems have been shown for many species. Suppressive effects (including hypoadditivity, see Figure 3) are observed more often than synergistic interactions (Cromarty and Derby 1998; Ochieng et al. 2002; Duchamp-Viret et al. 2003; Rospars et al. 2008; Hillier and Vickers 2011; Su et al. 2012). Suppressive mixture effects are also observed perceptually, and some of these could be linked to ORN physiology (Bell et al. 1987; Brodin et al. 2009; Chaput et al. 2012). Some of these suppressive mixture effects may arise from agonists and antagonists competing for a common receptor-binding site (Araneda et al. 2000; Oka et al. 2004). Our data also show an example of likely agonist competition, resulting in suppressive effects for all 3 binary mixtures tested. These

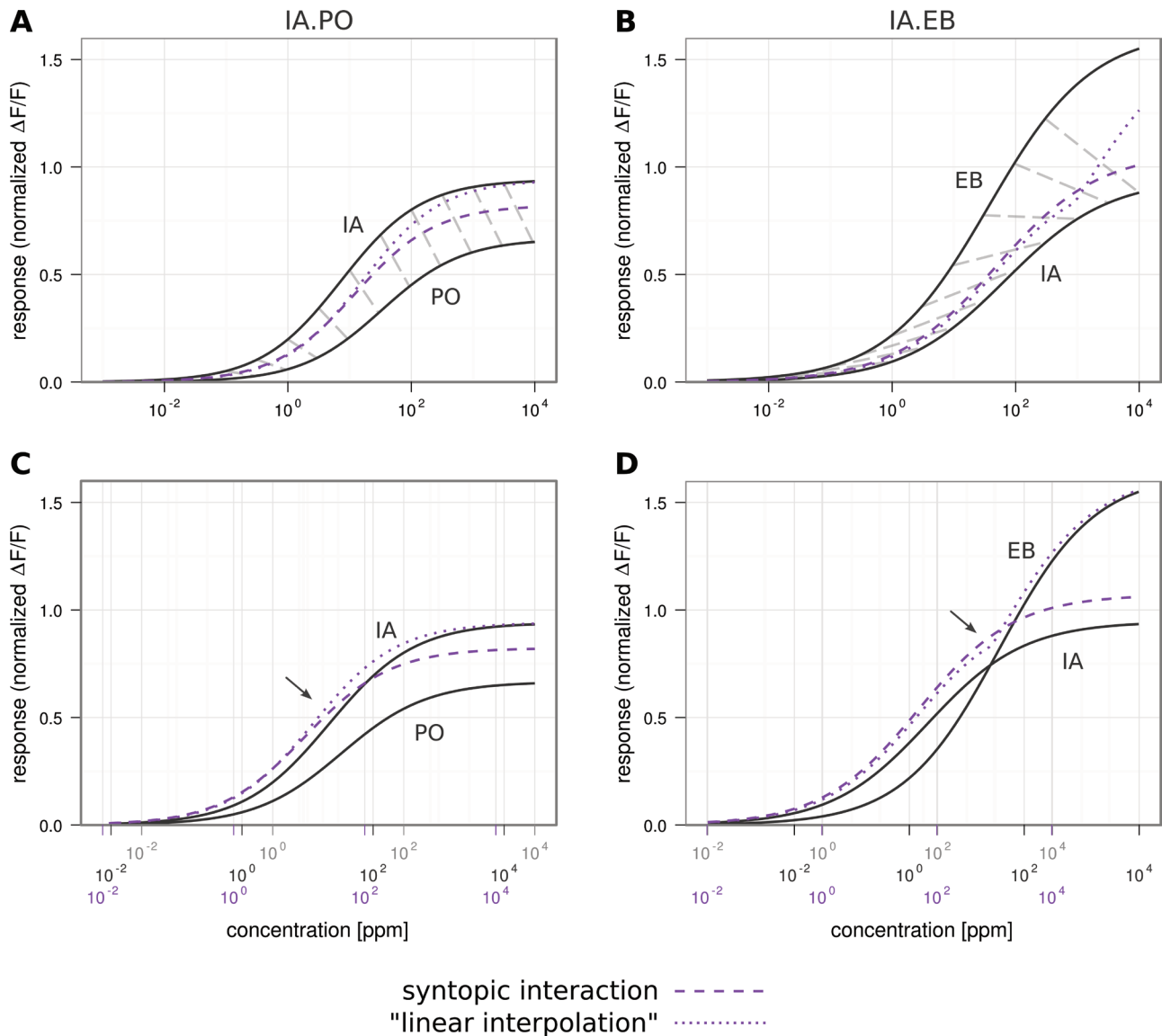


Figure 5 Mixture dose–response curves estimated for banana ratios. **A** and **B** Dark gray curves are the individual components IA and PO or EB, mixture curves in purple show predictions for syntopic interaction (dashed; Rospars et al., 2008) and for “linear interpolation” (dotted; Tabor et al., 2004). Light gray dashed lines in A and B connect corresponding points on the single compound curves according to their ratio in banana scent. C and D Data as in A and B but shifted so that corresponding single concentrations in the “banana ratio” and the resulting mixture are aligned vertically. Note that “linear interpolation” leads to a “kink” in the predicted dose–response curve in B and D. Arrows indicate where syntopic interaction and linear interpolation start to diverge with increasing concentration. This figure appears in color on the online version of this issue.

effects were fully explained by a model of syntopic interaction. Syntopic interaction describes the competition of 2 agonistic ligands for binding at a common or 2 overlapping receptor-binding sites (Neubig et al. 2003). Syntopic interaction leads to hypoaddivitivity or stronger suppressive effects at high concentration, whereas those competitive effects are absent at low concentrations with sufficient free binding sites where mixture responses match “linear interpolations” of their component responses (modeled responses in Figure 5).

The model for syntopic interaction is sufficient to explain the data that we measured. Nevertheless, this does not exclude that under other conditions, either for different

odors or other receptor cells, additional mechanisms of mixture interactions may occur. Such mechanisms could include multiple binding sites on 1 receptor, multiple second-messenger cascades, multiple receptors on 1 cell (e.g., the receptor cell studied here also expresses receptor dOr22b in addition to dOr22a although no active role for dOr22b has been shown yet), or interactions between neurons within 1 sensillum (e.g., ephaptic effects; Boekhoff et al. 1994; Cromarty and Derby 1997; Dobritsa et al. 2003; Vermeulen and Rospars 2004; French et al. 2011; Su et al. 2012). Some receptor cells show inhibitory responses to some odorants (antagonistic ligands), in which cases mixture interactions

need to be analyzed and modeled differently (Boekhoff et al. 1994; Kang and Caprio 1997; de Bruyne et al. 1999, 2001; Duchamp-Viret et al. 2003; Schuckel et al. 2009; Turner and Ray 2009).

dOr22a has a broad response profile with strong responses to many fruity odors, increasing the likelihood that mixture interactions occur in a natural environment. In more selective receptors, for example, dOr92a with 2,3-butanedione as dominant ligand (Galizia et al. 2010), syntopic interactions may not be relevant under natural conditions. However, even dOr92a has several weak ligands, so that this scenario needs to be tested specifically.

Syntopic interactions may also help the brain to create odor-concentration invariance. For example, a fruit fly that smells a banana should be able to identify this banana also when the scent gets stronger as it approaches the source. Odor-concentration invariance has been shown in behavior and physiology for different species and sequential ORN recruitment, and network effects in the brain are thought to underlie this capacity (Sachse and Galizia 2003; Uchida and Mainen 2007; Root et al. 2008; Asahina et al. 2009; Cleland et al. 2012). Generally, the dose–response curve to an odor follows a sigmoidal shape. However, in the absence of interactions, “linear interpolation” predicts that dose–response curves become less predictable because of the occurrence of “kinks” as in the calculated IA.EB mixture response curve (Figure 5). With syntopic interaction, however, responses to mixtures follow sigmoidal dose–response curves just as single compounds, so that the brain can use the same algorithms for concentration invariance for all odors, be they pure substances or mixtures.

Furthermore syntopic interaction helps to set the working range of receptors. The single receptor measured in this study is only a small part of the whole ensemble that consists of all the activated and nonactivated ORNs in response to an odor. In olfactory brain areas like the antennal lobe and the olfactory bulb, this ensemble response is shaped by a lateral network generating further mixture interactions (Giraudet et al. 2002; Sachse and Galizia 2002; Tabor et al. 2004; Silbering and Galizia 2007; Olsen and Wilson 2008; Root et al. 2008; Kuebler et al. 2011). If responses to mixture components would add up linearly (“linear interpolation”), many naturally occurring odors with tens or hundreds of components might quickly lead to saturated receptor cell output, thus reducing the coding capacity of the system. Our data strengthen the view that when studying mixture processing in brain networks, syntopic interaction at the periphery needs to be taken into account, even in the absence of chemical or physiological interactions.

The majority of odors consist of many chemical substances that occur together. The scent of banana, for example, was reported to contain 152 components, and Jordán et al. (2001) identified 26 substances in the headspace of fresh fruit. Is any of these the “main component” of banana, or is banana only

created by the characteristic mixture? To humans, the most concentrated component in banana (HE) smells like green apple. Following the components in order of concentration, we have to reach IA (rank 7, Figure 1) to find a substance that by itself reminds us of banana, even though we are by no means anosmic to the higher ranked components (Jordán et al. 2001). Honeybees have been shown to learn mixtures *via* the selection of a few key components rather than learning the full bouquet (Reinhard et al. 2010). Thus, at least in some cases, certain mixture components are more salient than others, which raises the question about the responsible mechanisms. Here we show a case study where an effect similar to key component selection happens at receptor neuron level, by syntopic interaction. In this example, the *Drosophila* receptor dOr22a “perceives” the banana-like mixture and its intermediate component IA as being equal even though there are both better and more concentrated ligands in the mixture.

Supplementary material

Supplementary material can be found at <http://www.chemse.oxfordjournals.org/>

Funding

This work was supported by the German Research Council [GA524/7] and the German Ministry of Education and Research [01GQ0931].

Acknowledgments

We thank Sheree Pfeiffer for help with the measurements.

References

- Araneda RC, Kini AD, Firestein S. 2000. The molecular receptive range of an odorant receptor. *Nat Neurosci.* 3(12):1248–1255.
- Asahina K, Louis M, Piccinotti S, Vosshall LB. 2009. A circuit supporting concentration-invariant odor perception in *Drosophila*. *J Biol.* 8(1):9.
- Bell GA, Laing DG, Panhuber H. 1987. Odour mixture suppression: evidence for a peripheral mechanism in human and rat. *Brain Res.* 426(1):8–18.
- Boekhoff I, Michel WC, Breer H, Ache BW. 1994. Single odors differentially stimulate dual second messenger pathways in lobster olfactory receptor cells. *J Neurosci.* 14:3304–3309.
- Brodin M, Laska M, Olsson MJ. 2009. Odor interaction between Bourgeonal and its antagonist undecanal. *Chem Senses.* 34(7):625–630.
- Chaput MA, El Mountassir F, Atanasova B, Thomas-Danguin T, Le Bon AM, Perrut A, Ferry B, Duchamp-Viret P. 2012. Interactions of odorants with olfactory receptors and receptor neurons match the perceptual dynamics observed for woody and fruity odorant mixtures. *Eur J Neurosci.* 35(4):584–597.
- Cleland TA, Chen S-YT, Hozer KW, Ukatu HN, Wong KJ, Zheng F. 2012. Sequential mechanisms underlying concentration invariance in biological olfaction. *Front Neuroeng.* 4:1–12.

- Cometto-Muñiz JE, Cain WS, Abraham MH. 2003. Quantification of chemical vapors in chemosensory research. *Chem Senses*. 28(6):467–477.
- Cromarty SI, Derby CD. 1997. Multiple excitatory receptor types on individual olfactory neurons: implications for coding of mixtures in the spiny lobster. *J Comp Physiol A*. 180(5):481–491.
- Cromarty SI, Derby CD. 1998. Inhibitory receptor binding events among the components of complex mixtures contribute to mixture suppression in responses of olfactory receptor neurons of spiny lobsters. *J Comp Physiol A*. 183(6):699–707.
- de Bruyne M, Clyne PJ, Carlson JR. 1999. Odor coding in a model olfactory organ: the *Drosophila* maxillary palp. *J Neurosci*. 19:4520–4532.
- de Bruyne M, Foster K, Carlson JR. 2001. Odor Coding in the *Drosophila* Antenna. *Neuron*. 30:537–552.
- Dobritsa AA, van der Goes van Naters W, Warr CG, Steinbrecht RA, Carlson JR. 2003. Integrating the molecular and cellular basis of odor coding in the *Drosophila* antenna. *Neuron*. 37(5):827–841.
- Duchamp-Viret P, Duchamp A, Chaput MA. 2003. Single olfactory sensory neurons simultaneously integrate the components of an odour mixture. *Eur J Neurosci*. 18(10):2690–2696.
- French AS, Torkkeli PH, Schuckel J. 2011. Dynamic characterization of *Drosophila* antennal olfactory neurons indicates multiple opponent signaling pathways in odor discrimination. *J Neurosci*. 31(3):861–869.
- Galizia CG, Münch D, Strauch M, Nissler A, Ma S. 2010. Integrating heterogeneous odor response data into a common response model: A DoOR to the complete olfactome. *Chem Senses*. 35(7):551–563.
- Giraudet P, Berthommier F, Chaput M. 2002. Mitral cell temporal response patterns evoked by odor mixtures in the rat olfactory bulb. *J Neurophysiol*. 88(2):829–838.
- Hallem EA, Carlson JR. 2006. Coding of odors by a receptor repertoire. *Cell*. 125(1):143–160.
- Hallem EA, Ho MG, Carlson JR. 2004. The molecular basis of odor coding in the *Drosophila* antenna. *Cell*. 117(7):965–979.
- Hillier NK, Vickers NJ. 2011. Mixture interactions in moth olfactory physiology: examining the effects of odorant mixture, concentration, distal stimulation, and antennal nerve transection on sensillar responses. *Chem Senses*. 36(1):93–108.
- Ignell R, Root CM, Birse RT, Wang JW, Nässel DR, Winther AM. 2009. Presynaptic peptidergic modulation of olfactory receptor neurons in *Drosophila*. *Proc Natl Acad Sci USA*. 106(31):13070–13075.
- Jinks A, Laing DG. 2001. The analysis of odor mixtures by humans: evidence for a configurational process. *Physiol Behav*. 72(1-2):51–63.
- Johnson BA, Ong J, Leon M. 2010. Glomerular activity patterns evoked by natural odor objects in the rat olfactory bulb are related to patterns evoked by major odorant components. *J Comp Neurol*. 518(9):1542–1555.
- Jordán MJ, Tandon K, Shaw PE, Goodner KL. 2001. Aromatic profile of aqueous banana essence and banana fruit by gas chromatography-mass spectrometry (GC-MS) and gas chromatography-olfactometry (GC-O). *J Agric Food Chem*. 49(10):4813–4817.
- Kang J, Caprio J. 1997. In vivo responses of single olfactory receptor neurons of channel catfish to binary mixtures of amino acids. *J Neurophysiol*. 77(1):1–8.
- Knudsen JT, Tollsten L, Bergström LG. 1993. Floral scents—a checklist of volatile compounds isolated by head-space techniques. *Phytochemistry*. 33:253–280.
- Kuebler LS, Olsson SB, Weniger R, Hansson BS. 2011. Neuronal processing of complex mixtures establishes a unique odor representation in the moth antennal lobe. *Front Neural Circuits*. 5:7.
- Lei H, Vickers N. 2008. Central processing of natural odor mixtures in insects. *J Chem Ecol*. 34(7):915–927.
- Nakai J, Ohkura M, Imoto K. 2001. A high signal-to-noise Ca(2+) probe composed of a single green fluorescent protein. *Nat Biotechnol*. 19(2):137–141.
- Neubig RR, Spedding M, Kenakin T, Christopoulos A. 2003. International Union of Pharmacology Committee on Receptor Nomenclature and Drug Classification. XXXVIII. Update on terms and symbols in quantitative pharmacology. *Pharmacol Rev*. 55(4):597–606.
- Ochieng SA, Park KC, Baker TC. 2002. Host plant volatiles synergize responses of sex pheromone-specific olfactory receptor neurons in male *Helicoverpa zea*. *J Comp Physiol A Neuroethol Sens Neural Behav Physiol*. 188(4):325–333.
- Oka Y, Omura M, Kataoka H, Touhara K. 2004. Olfactory receptor antagonism between odorants. *EMBO J*. 23(1):120–126.
- Olsen SR, Wilson RI. 2008. Lateral presynaptic inhibition mediates gain control in an olfactory circuit. *Nature*. 452(7190):956–960.
- Pelz D. 2005. Functional Characterization of *Drosophila melanogaster* Olfactory Receptor Neurons. Freie Universität Berlin. http://www.diss.fu-berlin.de/diss/receive/FUDISS_thesis_000000001732.
- Pelz D, Roeske T, Syed Z, de Bruyne M, Galizia CG. 2006. The molecular receptive range of an olfactory receptor in vivo (*Drosophila melanogaster* Or22a). *J Neurobiol*. 66(14):1544–1563.
- Reinhard J, Sinclair M, Srinivasan MV, Claudianos C. 2010. Honeybees learn odour mixtures via a selection of key odorants. *PLoS ONE*. 5(2):e9110.
- Root CM, Masuyama K, Green DS, Enell LE, Nässel DR, Lee CH, Wang JW. 2008. A presynaptic gain control mechanism fine-tunes olfactory behavior. *Neuron*. 59(2):311–321.
- Rospars JP, Lansky P, Chaput M, Duchamp-Viret P. 2008. Competitive and noncompetitive odorant interactions in the early neural coding of odorant mixtures. *J Neurosci*. 28(10):2659–2666.
- Sachse S, Galizia CG. 2002. Role of inhibition for temporal and spatial odor representation in olfactory output neurons: a calcium imaging study. *J Neurophysiol*. 87(2):1106–1117.
- Sachse S, Galizia CG. 2003. The coding of odour-intensity in the honeybee antennal lobe: local computation optimizes odour representation. *Eur J Neurosci*. 18(8):2119–2132.
- Schuckel J, Torkkeli PH, French AS. 2009. Two interacting olfactory transduction mechanisms have linked polarities and dynamics in *Drosophila melanogaster* antennal basiconic sensilla neurons. *J Neurophysiol*. 102(1):214–223.
- Silbering AF, Galizia CG. 2007. Processing of odor mixtures in the *Drosophila* antennal lobe reveals both global inhibition and glomerulus-specific interactions. *J Neurosci*. 27(44):11966–11977.
- Stensmyr MC, Giordano E, Balloi A, Angioy AM, Hansson BS. 2003. Novel natural ligands for *Drosophila* olfactory receptor neurones. *J Exp Biol*. 206:715–724.
- Su CY, Menuz K, Reisert J, Carlson JR. 2012. Non-synaptic inhibition between grouped neurons in an olfactory circuit. *Nature*. 492(7427):66–71.
- Tabor R, Yaksi E, Weislogel JM, Friedrich RW. 2004. Processing of odor mixtures in the zebrafish olfactory bulb. *J Neurosci*. 24(29):6611–6620.

- Turner SL, Ray A. 2009. Modification of CO₂ avoidance behaviour in *Drosophila* by inhibitory odorants. *Nature*. 461(7261):277–281.
- Uchida N, Mainen ZF. 2007. Odor concentration invariance by chemical ratio coding. *Front Syst Neurosci*. 1:3.
- Vermeulen A, Rospars JP. 2004. Why are insect olfactory receptor neurons grouped into sensilla? The teachings of a model investigating the effects of the electrical interaction between neurons on the transepithelial potential and the neuronal transmembrane potential. *Eur Biophys J*. 33(7):633–643.
- Wang JW, Wong AM, Flores J, Vosshall LB, Axel R. 2003. Two-photon calcium imaging reveals an odor-evoked map of activity in the fly brain. *Cell*. 112(2):271–282.